

Effective model for pure Yang-Mills theory on $\mathbb{T}^2 \times \mathbb{R}^2$ with Polyakov loops

Daiki Suenaga^{1,2,*} and Masakiyo Kitazawa^{3,4,5,†}

¹*Strangeness Nuclear Physics Laboratory, RIKEN Nishina Center, Wako 351-0198, Japan*

²*Research Center for Nuclear Physics, Osaka University, Ibaraki 567-0048, Japan*

³*Yukawa Institute for Theoretical Physics, Kyoto University, Kyoto, 606-8502 Japan*

⁴*J-PARC Branch, KEK Theory Center, Institute of Particle and Nuclear Studies, KEK, 319-1106 Japan*

⁵*Department of Physics, Osaka University, Toyonaka, Osaka, 560-0043 Japan*

(Dated: October 19, 2022)

We investigate the phase diagram and thermodynamics of $SU(N)$ pure Yang-Mills theory on a manifold $\mathbb{T}^2 \times \mathbb{R}^2$ with an effective model that includes two Polyakov loops along two compactified directions. We find that a rich phase structure can appear owing to the spontaneous breaking of two center symmetries for $N = 2$ and 3. Thermodynamic quantities are obtained in the model and compared with recent lattice results. It is shown that two Polyakov loops play significant roles in thermodynamics on $\mathbb{T}^2 \times \mathbb{R}^2$.

I. INTRODUCTION

Boundary conditions (BCs) in quantum field theory give rise to nontrivial modifications of the system. A renowned example is the Casimir effect in quantum electrodynamics [1], where the effect of the BC imposed by conductors is observable as the force acting on them [2, 3]. In the Matsubara formalism for thermal field theory, nonzero temperature (T) is introduced as the BC along the imaginary-time direction in the Euclidean spacetime. Various phenomena in thermal systems, such as phase transitions, thus can be viewed as those provoked by the BC.

In $SU(N)$ Yang-Mills (YM) theory, a BC introduces a new symmetry of the action, that is the center symmetry of the gauge group, Z_N , through the twist at the BC. YM theory at nonzero T thus has a Z_N symmetry. The deconfinement phase transition at nonzero T is characterized by the spontaneous breaking of this symmetry in the high temperature phase [4]. Observables that are not invariant under Z_N transformation are order parameters of this phase transition, and the Polyakov loop is a conventional choice among them [5].

When BCs along spatial directions are imposed into YM theory at nonzero T , the action has additional Z_N symmetries corresponding to the individual BCs. In such systems, therefore, phase transitions associated with the spontaneous breaking of individual Z_N symmetries are expected to occur with variations of T and spatial extent along the BCs. These phenomena, which are regarded as generalized Casimir effects in thermal systems, have been investigated from various motivations [6–19] including numerical simulations [20–28].

Recently, thermodynamics of $SU(3)$ YM theory with a periodic boundary condition (PBC) along one spatial

direction has been investigated in the lattice numerical simulation [26] using a technique based on the gradient flow [29–32]. With the BC, the pressure becomes anisotropic due to the violation of the rotational symmetry [33]. The numerical results in Ref. [26], however, show that in comparison with the free field theory the pressure anisotropy is remarkably suppressed until the spatial extent becomes significantly small near the critical temperature T_c . This result implies that the non-perturbative nature of the gauge field plays a crucial role in determining the response against the BC near T_c . It thus is also expected that the response can be used as a sensitive probe to understand the properties of the system.

In the present study, we investigate the phase transitions and thermodynamics of YM theory at nonzero T with BCs using an effective model. To be specific, throughout this paper we take the spatial dimension to be three and impose the PBC for one direction, say x , with the length L_x . Since the BC for the temporal direction is also periodic for gauge fields, this system is defined on a Euclidean manifold $\mathbb{T}^2 \times \mathbb{R}^2$ with two PBCs of length $L_\tau = 1/T$ and L_x . This system has two Z_N symmetries corresponding to two PBCs, and the phase transitions associated with their spontaneous breakings are expected to occur by varying L_τ and L_x . To describe these phase transitions simultaneously in an effective-model approach, the model must contain two order parameters.

For the YM theory on an infinite spatial volume without BCs, i.e. the theory on $\mathbb{S}^1 \times \mathbb{R}^3$, an effective model including the Polyakov loop as the order parameter has been proposed in Ref. [34]. In this model, the gauge field has a constant background field corresponding to the non-trivial expectation value of the Polyakov loop that is determined by the minimization of the free energy. It has been shown that thermodynamic quantities obtained on the lattice are qualitatively reproduced in the model. This result indicates that the Polyakov loop

* daiki.suenaga@riken.jp

† kitazawa@yukawa.kyoto-u.ac.jp

plays an important role in describing thermal properties of YM theory near T_c [35]. The idea has been improved in the literature by incorporating various effects, and also applied to QCD with dynamical fermions; see Ref. [36] as a review and references therein.

In the present study, to describe the theory on $\mathbb{T}^2 \times \mathbb{R}^2$ we extend these models by introducing two ‘‘Polyakov loops’’ along two compactified directions. Using this model, we investigate their roles in thermal properties of the system, especially the emergence of the anisotropic pressure. As the first trial of such an attempt, we consider a simple model composed of massless gauge field on the background field and a simple trial form for the Polyakov-loop potential. We investigate the phase diagram on the L_τ - L_x plane and thermodynamics for $N = 2$ and 3.

We show that an interesting phase structure with the second- and first-order phase-transition lines emerges for $N = 2$ and 3, respectively. We also calculate thermodynamic quantities on $\mathbb{T}^2 \times \mathbb{R}^2$ and compare them with the lattice results in Ref. [26]. In this analysis, we find that the thermodynamic quantities are significantly affected by the two Polyakov loops. We, however, find that our model fails to reproduce the lattice results even qualitatively. While the result obviously shows that our approach needs to be improved, we argue that such a modification is possible by changing the form of the potential term. Such a description of the YM theory on $\mathbb{T}^2 \times \mathbb{R}^2$ will in turn give us a deeper understanding of the theory on $\mathbb{S}^1 \times \mathbb{R}^3$. Although we do not attempt further modifications of the model in this exploratory study, possible directions will be discussed.

This article is organized as follows. In Sec. II, we introduce the effective model for the YM theory on $\mathbb{T}^2 \times \mathbb{R}^2$ including two types of the Polyakov loops. Besides, we explain its properties and present concrete expressions for $N = 2$ and $N = 3$. In Sec. III, we show our numerical results of the phase diagram on the L_τ - L_x plane for $N = 2$ and $N = 3$. In Sec. IV our model is compared to the lattice data of thermodynamic quantities obtained in Ref. [26] and some discussions on the role of the Polyakov loops are provided. Then, our present work is concluded in Sec. V.

II. MODEL

In the present study we introduce an effective model for describing the YM theory on the $\mathbb{T}^2 \times \mathbb{R}^2$ Euclidean manifold with PBCs. This system physically corresponds to a thermal system with the PBC along one spatial direction additionally, where the temporal length is related to temperature as $L_\tau = 1/T$. We suppose that the PBC is imposed along x direction and define the spatial extent by L_x , while the lengths along y and z directions are taken to be infinite.

A. Polyakov loops

The YM theory on $\mathbb{T}^2 \times \mathbb{R}^2$ is invariant under the center symmetries, which are denoted as $Z_N^{(\tau)}$ and $Z_N^{(x)}$. These symmetries can be spontaneously broken with variations of L_τ and L_x . To describe these phase transitions, we employ the Polyakov loops¹

$$\begin{aligned} P_\tau(x, \mathbf{r}_L) &= \frac{1}{N} \text{Tr} \left[\hat{P}_\tau(x, \mathbf{r}_L) \right] , \\ P_x(\tau, \mathbf{r}_L) &= \frac{1}{N} \text{Tr} \left[\hat{P}_x(\tau, \mathbf{r}_L) \right] , \end{aligned} \quad (1)$$

for the order parameters, where Tr means the trace over the gauge space and the Polyakov-loop matrices are defined by

$$\begin{aligned} \hat{P}_\tau(x, \mathbf{r}_L) &= \mathcal{P} \exp \left(i \int_0^{L_\tau} A_\tau(\tau, x, \mathbf{r}_L) d\tau \right) , \\ \hat{P}_x(\tau, \mathbf{r}_L) &= \mathcal{P} \exp \left(i \int_0^{L_x} A_x(\tau, x, \mathbf{r}_L) dx \right) . \end{aligned} \quad (2)$$

In Eq. (2), $A_\mu(\tau, x, \mathbf{r}_L)$ is the YM gauge field [$\mu = (x, y, z, \tau)$], \mathcal{P} stands for the path-ordering integral, and $\mathbf{r}_L = (y, z)$ represents the uncompactified two spatial variables.

The Polyakov loops P_τ and P_x are not invariant under $Z_N^{(\tau)}$ and $Z_N^{(x)}$, respectively, and are order parameters of the corresponding symmetries. It is also known that the thermal expectation value $\langle P_\tau \rangle$ is related to the free energy $F_q(x, \mathbf{r}_L)$ of a static test quark as [37]

$$e^{-L_\tau F_q(x, \mathbf{r}_L)} = N \langle P_\tau(x, \mathbf{r}_L) \rangle . \quad (3)$$

Therefore, $\langle P_\tau \rangle = 0$ corresponds to the confined phase in which F_q becomes infinite. In YM theory on $\mathbb{S}^1 \times \mathbb{R}^3$, this phase is realized as a low-temperature phase, while the deconfined phase with $\langle P_\tau \rangle \neq 0$ is realized at high T . These phases are separated by the second- and first-order phase transition for $N = 2$ and $N \geq 3$, respectively [4, 36, 38–43].

B. Model construction

For a simultaneous description of the spontaneous breakings of $Z_N^{(\tau)}$ and $Z_N^{(x)}$ on $\mathbb{T}^2 \times \mathbb{R}^2$, we construct an effective model including P_τ and P_x for their order parameters. To this end, we extend the ‘‘model-B’’ introduced in Ref. [34] that deals with a single Polyakov loop P_τ on $\mathbb{S}^1 \times \mathbb{R}^3$.

In Ref. [34], to represent a non-trivial value of P_τ the ‘‘mean-field’’ assumption is imposed, where the gauge

¹ The quantity that is conventionally called the Polyakov loop is P_τ . In this manuscript, however, we refer to both P_τ and P_x as the Polyakov loops for simplicity.

field has a constant background field. The free energy of the system consists of two parts; the first one is the one-loop perturbative contribution from the gauge field with the background field, and the other is a potential term that models non-perturbative effects leading to the confinement. The expectation value of P_τ is determined so as to minimize the free energy. It has been shown that the model can reproduce T dependence of thermodynamic quantities measured in lattice simulations qualitatively.

By extending this idea, we assume that the gauge field on $\mathbb{T}^2 \times \mathbb{R}^2$ has a constant background field

$$A_\tau(\tau, x, \mathbf{r}_L) = \frac{1}{L_\tau} \text{diag}[(\theta_\tau)_1, (\theta_\tau)_2, \dots, (\theta_\tau)_N], \quad (4)$$

$$A_x(\tau, x, \mathbf{r}_L) = \frac{1}{L_x} \text{diag}[(\theta_x)_1, (\theta_x)_2, \dots, (\theta_x)_N], \quad (5)$$

corresponding to the expectation values of P_τ and P_x . Substituting Eqs. (4) and (5) into Eq. (2), one obtains

$$(\hat{P}_c)_{jk} = \exp(i(\theta_c)_j) \delta_{jk}, \quad (6)$$

for $c = \tau, x$ and

$$P_c = \frac{1}{N} \sum_{j=1}^N \exp(i(\theta_c)_j). \quad (7)$$

Since \hat{P}_c is an element of $SU(N)$, the phase variables $\vec{\theta}_c = ((\theta_c)_1, \dots, (\theta_c)_N)$ satisfy

$$\sum_{j=1}^N (\theta_c)_j = 0 \pmod{2\pi}. \quad (8)$$

In Eqs. (4) and (5), the background field is assumed to have diagonal forms following Ref. [34]. In Ref. [34], the background field is introduced only for $A_\tau(\tau, x, \mathbf{r}_L)$ because P_x is irrelevant on $\mathbb{S}^1 \times \mathbb{R}^3$. In this case, $A_\tau(\tau, x, \mathbf{r}_L)$ can be diagonalized only with the gauge transformation. In contrast, the simultaneous diagonalization of $A_\tau(\tau, x, \mathbf{r}_L)$ and $A_x(\tau, x, \mathbf{r}_L)$ as in Eqs. (4) and (5) by using gauge degrees of freedom is not possible in general. However, since the purpose of the present study is to explore qualitative effects of P_τ and P_x on $\mathbb{T}^2 \times \mathbb{R}^2$, we employ the ansatz (4) and (5), which is a simple choice to realize non-trivial values of P_τ and P_x .

For later use, it is convenient to parametrize the phase variables $\vec{\theta}_\tau$ and $\vec{\theta}_x$ for $N = 2$ and $N = 3$ within the constraint (8). For $N = 2$, each phase is parametrized by a single parameter ϕ_c as

$$\vec{\theta}_c = (\phi_c, -\phi_c). \quad (9)$$

In this parametrization the Polyakov loops are given by

$$P_c = \cos \phi_c. \quad (10)$$

The non-perturbative vacuum where the center symmetries are restored is given by $\phi_c = \pi/2$. On the

other hand, the completely perturbative vacuum is realized with $\phi_c = 0$. We thus impose the range of ϕ_c as $0 \leq \phi_c \leq \pi/2$ for $N = 2$.

For $N = 3$, $\vec{\theta}_c$ has two degrees of freedom. The symmetric phase with $P_c = 0$ is realized, for example, at $\vec{\theta}_c = (2\pi/3, 0, -2\pi/3)$, while the perturbative vacuum corresponds to $\vec{\theta}_c = \vec{0}$. To connect these values, following Ref. [34, 36], we parametrize the phases as

$$\vec{\theta}_c = (\phi_c, 0, -\phi_c), \quad (11)$$

resulting in

$$P_c = \frac{1}{3}(1 + 2 \cos \phi_c), \quad (12)$$

with $0 \leq \phi_c \leq 2\pi/3$.

The one-loop free energy per unit volume with the background field (4) and (5) is calculated to be [42]

$$\begin{aligned} f_{\text{pert}}(\vec{\theta}_\tau, \vec{\theta}_x; L_\tau, L_x) &= \frac{2}{L_\tau L_x} \sum_{j,k=1}^N \left(1 - \frac{\delta_{jk}}{N}\right) \sum_{l_\tau, l_x} \int \frac{d^2 p_L}{(2\pi)^2} \\ &\times \ln \left[\left(\omega_\tau - \frac{(\Delta\theta_\tau)_{jk}}{L_\tau} \right)^2 + \left(\omega_x + \frac{(\Delta\theta_x)_{jk}}{L_x} \right)^2 + \mathbf{p}_L^2 \right], \end{aligned} \quad (13)$$

where the mass of the gauge field is assumed to vanish. In Eq. (13), $\omega_\tau = 2\pi l_\tau / L_\tau$ and $\omega_x = 2\pi l_x / L_x$ are the respective ‘‘Matsubara modes’’ with l_τ and l_x being integers. We have defined momenta for the uncompactified directions by $\mathbf{p}_L = (p_y, p_z)$, and the phase differences $(\Delta\theta_c)_{jk} = (\theta_c)_j - (\theta_c)_k$.

For a given set of (L_τ, L_x) , the minimum of Eq. (13) is at $\vec{\theta}_\tau = \vec{\theta}_x = \vec{0} \pmod{2\pi}$, which gives $P_\tau = P_x = 1$. Defining the expectation values of P_τ and P_x as the minimum of Eq. (13), therefore, the system is always in the deconfined phase. To model the confinement phase transition, we introduce a potential term of the Polyakov loops $f_{\text{pot}}(\vec{\theta}_\tau, \vec{\theta}_x; L_\tau, L_x)$, such that the total free energy per unit volume reads

$$\begin{aligned} f(\vec{\theta}_\tau, \vec{\theta}_x; L_\tau, L_x) &= f_{\text{pert}}(\vec{\theta}_\tau, \vec{\theta}_x; L_\tau, L_x) \\ &+ f_{\text{pot}}(\vec{\theta}_\tau, \vec{\theta}_x; L_\tau, L_x). \end{aligned} \quad (14)$$

Here, f_{pot} describes the non-perturbative effects that would have a dominant contribution at large L_τ or L_x . The specific form of f_{pot} will be determined later. The values of $\vec{\theta}_c$, and hence P_c , are determined so as to minimize Eq. (14).

C. One-loop free energy

With the parametrizations (9) and (11), the one-loop free energy (13) is transformed into the form that is more suitable for numerical analyses. After the manipulations

summarized in Appendix A with the regularization explained in Appendix B, one obtains

$$f_{\text{pert}} = -\frac{\pi^2}{15L_\tau^4} + \frac{4\phi_\tau^2(\phi_\tau - \pi)^2}{3\pi^2L_\tau^4} - \frac{\pi^2}{15L_x^4} + \frac{4\phi_x^2(\phi_x - \pi)^2}{3\pi^2L_x^4} - \frac{4}{\pi^2} \sum_{l_\tau, l_x=1}^{\infty} \frac{1 + 2\cos(2\phi_\tau l_\tau) \cos(2\phi_x l_x)}{X_{l_\tau, l_x}^4}, \quad (15)$$

for $N = 2$, while for $N = 3$ one has

$$f_{\text{pert}} = -\frac{8\pi^2}{45L_\tau^4} + \frac{8\phi_\tau^2(\phi_\tau - \pi)^2 + \phi_\tau^2(\phi_\tau - 2\pi)^2}{6\pi^2L_\tau^4} - \frac{8\pi^2}{45L_x^4} + \frac{8\phi_x^2(\phi_x - \pi)^2 + \phi_x^2(\phi_x - 2\pi)^2}{6\pi^2L_x^4} - \frac{8}{\pi^2} \sum_{l_\tau, l_x=1}^{\infty} \frac{1}{X_{l_\tau, l_x}^4} \left[1 + 2\cos(\phi_\tau l_\tau) \cos(\phi_x l_x) + \cos(2\phi_\tau l_\tau) \cos(2\phi_x l_x) \right], \quad (16)$$

with

$$X_{l_\tau, l_x} \equiv \sqrt{(l_\tau L_\tau)^2 + (l_x L_x)^2}. \quad (17)$$

In the limit $L_x \rightarrow \infty$, only the first two terms in Eqs. (15) and (16) that do not include $1/L_x$ survive. The form of f_{pert} in this limit reproduces that for $\mathbb{S}^1 \times \mathbb{R}^3$ [34]. The subleading terms with respect to $1/L_x$ come from the last double-sum term in Eq. (15) or (16). As discussed in Appendix A, the subleading term starts at the order $(L_\tau/L_x)^3$;

$$f_{\text{pert}} = \hat{f}_\infty(\vec{\theta}_\tau) \frac{1}{L_\tau^4} + \mathcal{O}(L_x^{-3}). \quad (18)$$

Note that odd-order terms of L_τ/L_x appear in this expansion, while Eqs. (15) and (16) apparently depend on L_τ/L_x only through $(L_\tau/L_x)^2$; see Appendix A.

D. Potential term

Next, we determine the form of f_{pot} . To this end let us first consider general properties of this term.

First, since the YM theory on $\mathbb{T}^2 \times \mathbb{R}^2$ is invariant under the exchange of the τ and x axes, f_{pot} should satisfy

$$f_{\text{pot}}(\vec{\theta}_\tau, \vec{\theta}_x; L_\tau, L_x) = f_{\text{pot}}(\vec{\theta}_x, \vec{\theta}_\tau; L_x, L_\tau). \quad (19)$$

Second, in the $L_\tau \rightarrow \infty$ ($T \rightarrow 0$) limit the system with the PBC would be in the confined phase irrespective of the value of L_x . We thus have

$$P_\tau = 0 \quad (L_\tau \rightarrow \infty). \quad (20)$$

By exchanging the τ and x axes, one also obtains

$$P_x = 0 \quad (L_x \rightarrow \infty). \quad (21)$$

It is worth emphasizing that the limiting value of P_c in these limits is not the perturbative one $P_c = 1$. However,

the values of P_τ and P_x in these limits are irrelevant in the sense that they do not affect the property of the system since effects of the BC should be negligible. In fact, the background field A_c in Eqs. (4) and (5) vanishes in the $L_c \rightarrow \infty$ limit irrespective of the value of $\vec{\theta}_c$.

Third, since the system approaches $\mathbb{S}^1 \times \mathbb{R}^3$ in the limit $L_x \rightarrow \infty$, the potential term should approach the one on $\mathbb{S}^1 \times \mathbb{R}^3$, i.e.

$$f_{\text{pot}}(\vec{\theta}_\tau, \vec{\theta}_x; L_\tau, L_x) \xrightarrow{L_x \rightarrow \infty} f_{\text{pot}}^{\mathbb{S}^1 \times \mathbb{R}^3}(\vec{\theta}_\tau; L_\tau), \quad (22)$$

where $f_{\text{pot}}^{\mathbb{S}^1 \times \mathbb{R}^3}(\vec{\theta}; L)$ is the potential term for the effective model for $\mathbb{S}^1 \times \mathbb{R}^3$ with a single Polyakov loop P_τ . Equation (22) means that $\vec{\theta}_x$ dependence in f_{pot} exists at the subleading order of L_τ/L_x , and this contribution leads to Eq. (21). This implies that the $\vec{\theta}_x$ dependence in f_{pot} must surpass the perturbative contributions f_{pert} which is of order $(L_\tau/L_x)^3$ as in Eq. (18), and hence the former should be weaker than the power of $(L_\tau/L_x)^3$. From Eq. (19), one obtains the same conclusion for the limit $L_\tau \rightarrow \infty$, i.e.

$$f_{\text{pot}}(\vec{\theta}_\tau, \vec{\theta}_x; L_\tau, L_x) \xrightarrow{L_\tau \rightarrow \infty} f_{\text{pot}}^{\mathbb{S}^1 \times \mathbb{R}^3}(\vec{\theta}_x; L_x), \quad (23)$$

with $\vec{\theta}_\tau$ dependence satisfying Eq. (20). When one constructs an effective model on $\mathbb{T}^2 \times \mathbb{R}^2$ as an extension of that developed for $\mathbb{S}^1 \times \mathbb{R}^3$, Eqs. (22) and (23) are constraints for f_{pot} .

In the model-B of Ref. [34], as an effective model on $\mathbb{S}^1 \times \mathbb{R}^3$ the form of the potential term motivated by the Haar measure in the strong-coupling expansion

$$f_{\text{pot}}^{\mathbb{S}^1 \times \mathbb{R}^3}(\vec{\theta}_\tau; L) = -\frac{1}{LR^3} \ln \left[\prod_{j < k} \sin^2 \left(\frac{(\Delta\theta_\tau)_{jk}}{2} \right) \right] \quad (24)$$

has been employed in combination with f_{pert} for the massless gauge field. Here, the quantity R having a mass dimension of -1 is understood as a typical length scale for the confinement; when $R \ll L_\tau$, the potential term dominates over f_{pert} and the confined phase is realized.

In the present study, we employ Eq. (24) as the form of $f_{\text{pot}}^{\mathbb{S}^1 \times \mathbb{R}^3}$ and introduce $f_{\text{pot}}(\vec{\theta}_\tau, \vec{\theta}_x; L_\tau, L_x)$ so as to satisfy Eqs. (22) and (23). There are, of course, infinitely many possible forms of $f_{\text{pot}}(\vec{\theta}_\tau, \vec{\theta}_x; L_\tau, L_x)$ within the constraint. Among them, in this exploratory study, we employ a simple separable ansatz

$$\begin{aligned} f_{\text{pot}}(\vec{\theta}_\tau, \vec{\theta}_x; L_\tau, L_x) &= f_{\text{pot}}^{\mathbb{S}^1 \times \mathbb{R}^3}(\vec{\theta}_\tau; L_\tau) + f_{\text{pot}}^{\mathbb{S}^1 \times \mathbb{R}^3}(\vec{\theta}_x; L_x) \\ &= -\frac{1}{L_\tau R^3} \ln \left[\prod_{j < k} \sin^2 \left(\frac{(\Delta\theta_\tau)_{jk}}{2} \right) \right] \\ &\quad - \frac{1}{L_x R^3} \ln \left[\prod_{j < k} \sin^2 \left(\frac{(\Delta\theta_x)_{jk}}{2} \right) \right]. \end{aligned} \quad (25)$$

We note that Eq. (25) satisfies all the conditions (19)–(23).

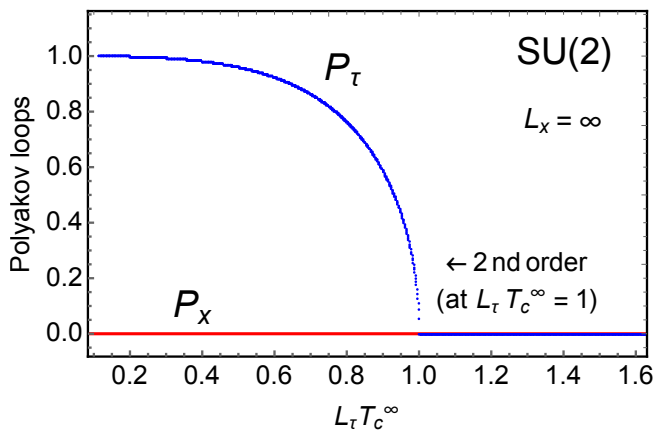


FIG. 1. L_τ dependence of P_τ (blue) and P_x (red) at $L_x \rightarrow \infty$ for $N = 2$. There exists a second-order phase transition at $L_\tau T_c^\infty = 1$ with the critical temperature $T_c^\infty \approx 1/(0.874R)$. The spatial Polyakov loop P_x is always zero.

With the phase variables in Eqs. (9) and (11), Eq. (25) is reduced to

$$f_{\text{pot}} = -\frac{1}{L_\tau R^3} \ln(\sin^2 \phi_\tau) - \frac{1}{L_x R^3} \ln(\sin^2 \phi_x), \quad (26)$$

for $N = 2$ and

$$f_{\text{pot}} = -\frac{1}{L_\tau R^3} \ln \left[\left(\sin^4 \frac{\phi_\tau}{2} \right) (\sin^2 \phi_\tau) \right] - \frac{1}{L_x R^3} \ln \left[\left(\sin^4 \frac{\phi_x}{2} \right) (\sin^2 \phi_x) \right], \quad (27)$$

for $N = 3$.

III. PHASE DIAGRAM

In this section, we investigate the model introduced in the previous section focusing on the behavior of the order parameters and the phase diagram on the L_τ - L_x plane for $N = 2, 3$.

A. $N = 2$

In this subsection we explore the case for $N = 2$. In Fig. 1 we first show the L_τ dependence of the Polyakov loops at $L_x \rightarrow \infty$ for $N = 2$ in order to check the behavior on $\mathbb{S}^1 \times \mathbb{R}^3$ [34]. The blue and red curves represent the temporal and spatial Polyakov loops P_τ and P_x , respectively. As can be seen, P_τ experiences a phase transition. As in Appendix C, it is shown from the Ginzburg-Landau analysis that this is a second-order phase transition with the critical temperature $T_c^\infty = 1/((2/3)^{1/3}R) \approx 1/(0.874R)$. The $Z_2^{(\tau)}$ symmetry is broken for $L_\tau T_c^\infty \leq 1$ corresponding to the deconfinement. On the other hand, P_x is always zero in $L_x \rightarrow \infty$ limit as in Eq. (21).

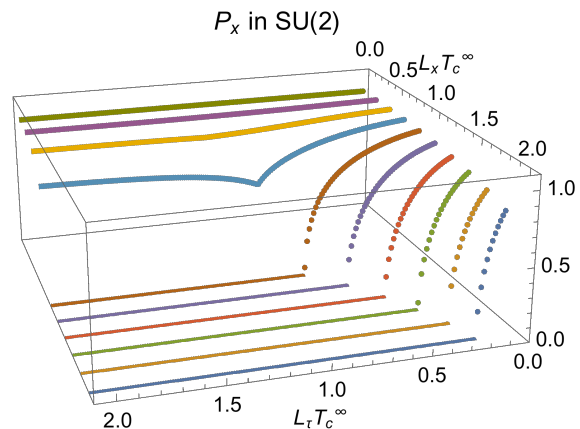
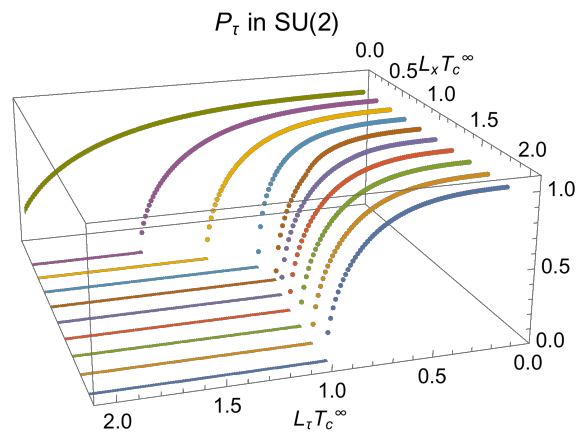


FIG. 2. L_τ dependences of P_τ (top panel) and P_x (bottom panel) at several L_x for $N = 2$.

In Fig. 2 we display the L_τ dependence of P_τ (top panel) and P_x (bottom panel) for several values of L_x . The upper panel indicates that the deconfinement phase transition on $\mathbb{S}^1 \times \mathbb{R}^3$ persists even for finite L_x . The critical value of L_τ first decreases with decreasing L_x , but it suddenly starts increasing at the symmetric point $L_\tau = L_x$. Meanwhile, the bottom panel shows that a phase with the spontaneous breaking of $Z_2^{(x)}$ symmetry appears at small L_τ , and the critical value of L_τ for this phase transition becomes larger with decreasing L_x . Moreover, $Z_2^{(x)}$ symmetry is mostly broken for sufficiently small L_x ($L_x T_c^\infty \lesssim 0.9$).

While it is analytically shown that the phase transition at $L_x \rightarrow \infty$ is of second order, it is difficult to obtain a definite conclusion analytically for finite L_x . Our numerical results, however, strongly suggest that the order parameters change continuously and thus the phase transitions are of second order for any value of L_x . To see this, in Fig. 3 we focus on the symmetric case $L_x = L_\tau = L$ and show the L dependence of the Polyakov loops that behave $P = P_\tau = P_x$ in this case. As shown in Appendix C, provided that the phase transition is of second

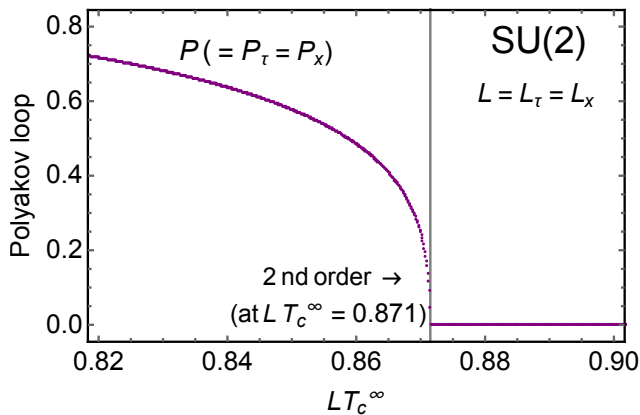


FIG. 3. Polyakov loops $P(\equiv P_\tau = P_x)$ for the symmetric case $L = L_\tau = L_x$ for $N = 2$ in the vicinity of the transition point. The second-order transition is found at $LT_c^\infty \approx 0.871$. The vertical line corresponds to the analytic solution for the second-order transition evaluated in Eq. (28).

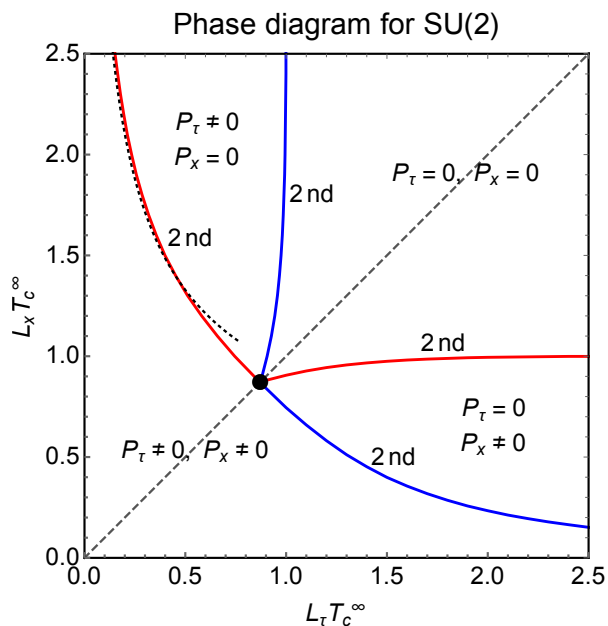


FIG. 4. Phase diagram on the L_τ - L_x plane for $N = 2$. The blue (red) line separates $P_\tau = 0$ and $P_\tau \neq 0$ ($P_x = 0$ and $P_x \neq 0$). The dashed gray line stands for $L_\tau = L_x$, and the black dot is the transition point in Fig. 3. All phase transitions are of second order. The dotted line shows the asymptotic formula (C10).

order it occurs at

$$LT_c^\infty = (2 \ln 2 / \pi)^{1/3} RT_c^\infty = (3 \ln 2 / \pi)^{1/3} \approx 0.871 \quad (28)$$

The figure suggests that the order parameter becomes nonzero at this point without discontinuity. The analytic solution (28) is denoted by the vertical line in the figure.

These results are well summarized as the phase diagram on the L_τ - L_x plane shown in Fig. 4. The blue (red) curve separates $P_\tau = 0$ and $P_\tau \neq 0$ ($P_x = 0$ and

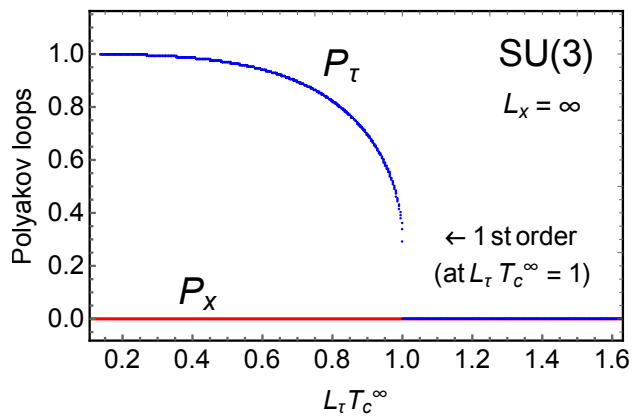


FIG. 5. L_τ dependence of P_τ (blue) and P_x (red) at $L_x \rightarrow \infty$ for $N = 3$. The temporal Polyakov loop P_τ shows a first-order phase transition at $T_c^\infty \approx 1/(0.733R)$.

$P_x \neq 0$). The dashed gray line stands for $L_\tau = L_x$, and the black dot represents the transition point on this line.

Finally, let us investigate the fate of the red line that separates $P_x \neq 0$ and $P_x = 0$ in the limit $(L_x, L_\tau) \rightarrow (\infty, 0)$. As discussed in Appendix C, provided the second-order transition the limiting behavior of this line is given as in Eq. (C10). In Fig. 4, we show Eq. (C10) by the dotted line. The line agrees well for $LT_c^\infty \gtrsim 1.3$.

B. $N = 3$

Next, we explore the $N = 3$ case. Depicted in Fig. 5 is the L_τ dependence of P_τ and P_x at $L_x \rightarrow \infty$. The blue and red curves represent P_τ and P_x , respectively. One sees from the figure that the deconfined phase is realized for $L_\tau = 1/T_c^\infty$, with the critical temperature numerically estimated as $T_c^\infty \approx 1/(0.733R)$. Unlike $N = 2$, the numerical result shows that P_τ has a clear discontinuity at this point, which means that the phase transition is of first order. As discussed in Appendix C, this result is analytically confirmed by the Ginzburg-Landau analysis.

In Fig. 6 we display the L_τ dependence of P_τ (top panel) and P_x (bottom panel) at several L_x . At larger L_x , the top panel implies that the first-order phase transition of P_τ observed at $L_x \rightarrow \infty$ persists to $L_x T_c^\infty \sim 1$. One also finds that both P_τ and P_x change discontinuously at the identical transition point. The first-order phase transition then ceases to exist at adequately small L_x ($L_x T_c^\infty \lesssim 1$).

To see the order of the phase transition, in Fig. 7 we show the $L(=L_\tau=L_x)$ dependence of $P(=P_\tau=P_x)$ for the symmetric case $L_\tau=L_x$ around the transition point. As shown in the figure, P changes discontinuously at $LT_c^\infty \approx 0.991$ meaning that the transition is of first order even at the symmetric point. Thus, we conclude that the transition is always of first order for $N = 3$.

Finally, we show the phase diagram on the L_τ - L_x plane in Fig. 8. As explained above the first-order phase

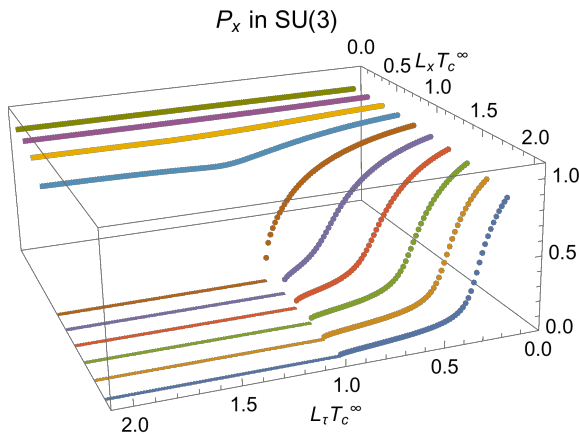
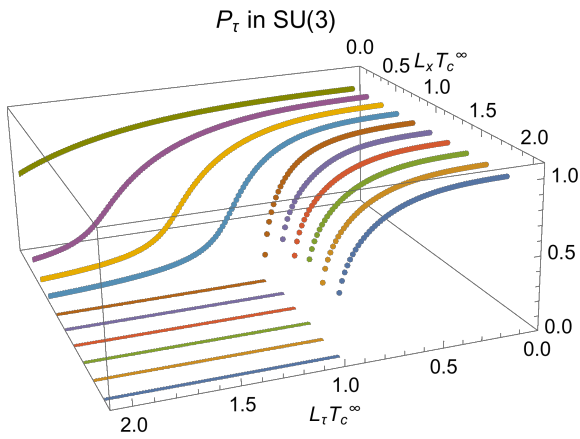


FIG. 6. L_τ dependences of P_τ (top panel) and P_x (bottom panel) at several L_x for $N = 3$.

transitions of P_τ and P_x occur simultaneously. This transition is shown by the purple line. The dashed gray line stands for $L_\tau = L_x$, and the black dot represents the transition point on this line. Note that P_x approaches zero for $L_x \rightarrow \infty$ such that the condition in Eq. (21) is satisfied, while the discontinuity of P_x does exist at the first-order transition point.

IV. THERMODYNAMICS

In this section, we investigate L_τ and L_x dependence of thermodynamic quantities on $\mathbb{T}^2 \times \mathbb{R}^2$ and study the impact of P_τ and P_x on them.

An important feature of the thermodynamics on $\mathbb{T}^2 \times \mathbb{R}^2$ is that the pressure becomes anisotropic because of the violation of rotational symmetry due to the BC [26]. In such systems, the stress tensor σ_{ij} with $i, j = x, y, z$ should be used in place of the pressure to represent the force acting on the surface. The stress tensor is equivalent with the spatial components of the energy-momentum tensor T_ν^μ up to the overall sign. The spatial compo-

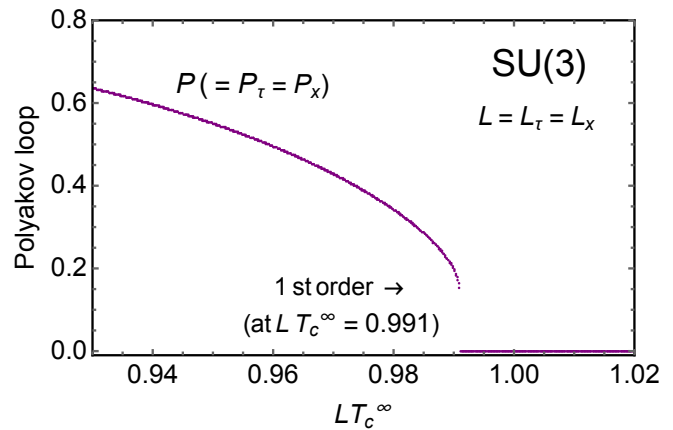


FIG. 7. L ($\equiv L_\tau = L_x$) dependence of the Polyakov loop P ($\equiv P_\tau = P_x$) for $N = 3$ in the vicinity of the phase transition point. The first-order transition occurs at $L T_c^\infty \approx 0.991$.

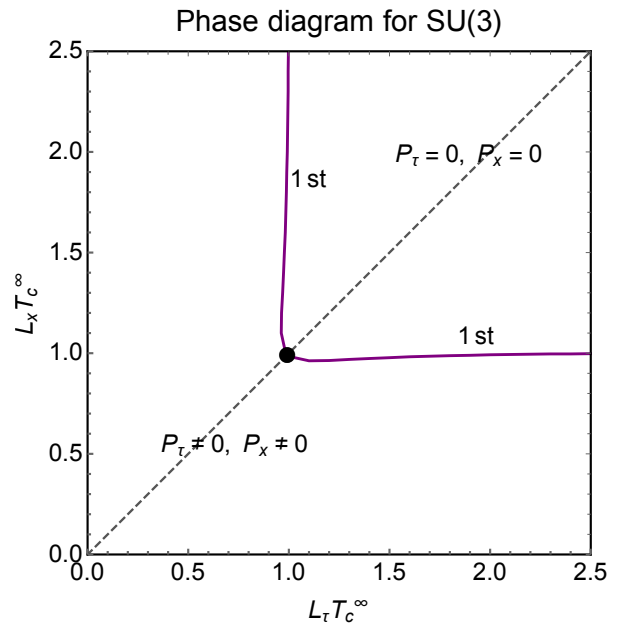


FIG. 8. Phase diagram on the $L_\tau - L_x$ plane for $N = 3$. The solid line shows the first-order phase transition.

nents of T_ν^μ , and thus σ_{ij} , have off-diagonal components in general. However, in our setting that imposes a PBC along x direction, due to the parity symmetry the energy-momentum tensor in the Minkowski space is given by the diagonal form as

$$T_\nu^\mu = \text{diag}(\epsilon, p_x, p_y, p_z), \quad (29)$$

where ϵ is the energy density and p_i represents the pressure for each direction. Because of the rotational symmetry around x axis $p_y = p_z$ is satisfied, but p_x can be different from p_y and p_z .

The values of ϵ , p_x and p_z in our model are obtained

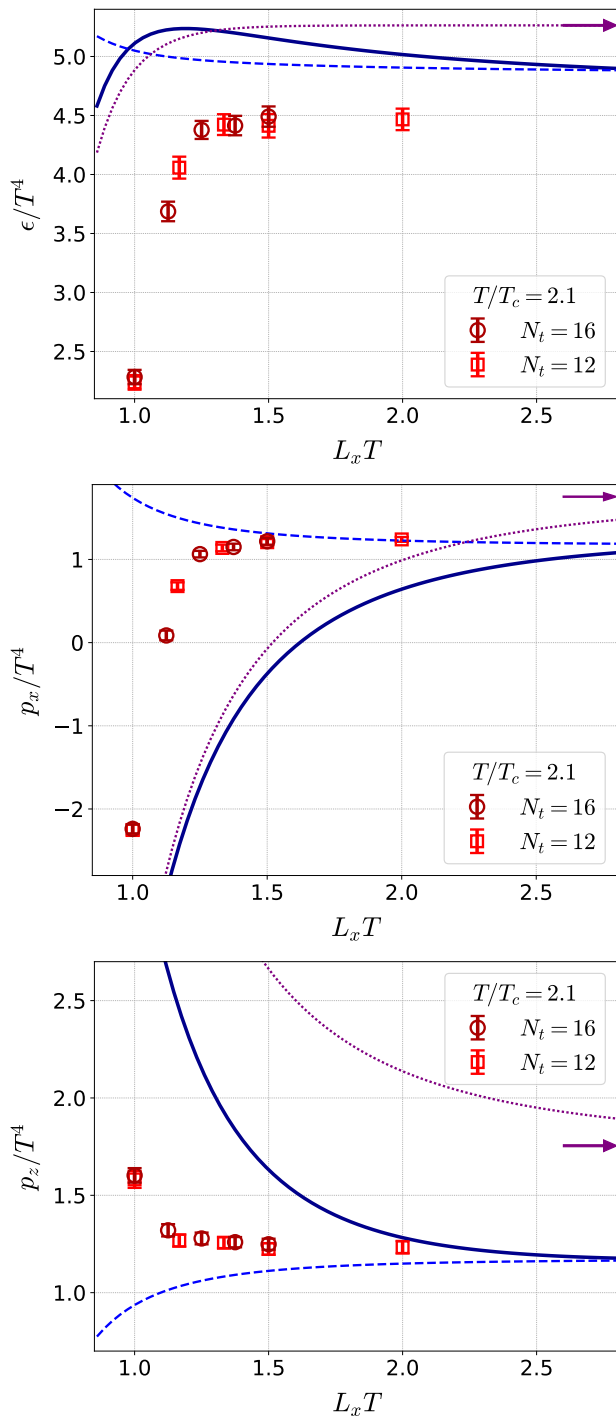


FIG. 9. Comparison of energy density ϵ and pressures p_x and p_z between our model (solid lines) and the lattice data in Ref. [26] with $N_t = 16$ (circles) and 12 (squares). The dashed lines show the results with fixed values of P_x and P_t given in the $L_x \rightarrow \infty$ limit. The dotted lines are the results in the massless free theory and their limiting values for $L_x T \rightarrow \infty$ are shown by the arrows.

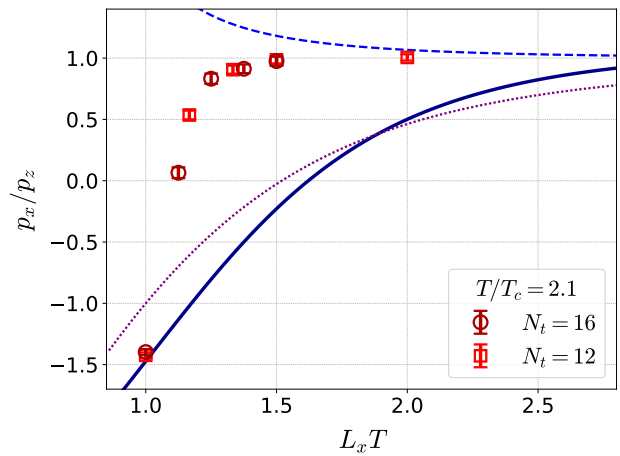


FIG. 10. Pressure ratio p_x/p_z . The meanings of the symbols are the same as Fig. 9.

from the free energy as

$$\begin{aligned}\epsilon &= \frac{L_\tau}{\mathcal{V}} \frac{\partial}{\partial L_\tau} \mathcal{V} f, \\ p_x &= -\frac{L_x}{\mathcal{V}} \frac{\partial}{\partial L_x} \mathcal{V} f, \\ p_z &= -\frac{L_z}{\mathcal{V}} \frac{\partial}{\partial L_z} \mathcal{V} f,\end{aligned}\quad (30)$$

where we have introduced the Euclidean four dimensional volume $\mathcal{V} = L_\tau L_x L_y L_z$ and temporarily assumed that the lengths for y and z directions, L_y and L_z , are finite.

In Fig. 9, we show the $L_x T (= L_x/L_\tau)$ dependence of ϵ , p_x and p_z obtained in our model for $N = 3$ at $T/T_c^\infty = 1/(L_\tau T_c^\infty) = 2.10$ by the solid blue lines. In the figure, same quantities calculated in the massless free theory are shown by the dotted lines for comparison. Their limiting values for $L_x T \rightarrow \infty$ are shown by the arrows. In the figure, we also plot these quantities in $SU(3)$ YM theory on $\mathbb{T}^2 \times \mathbb{R}^2$ for the same T obtained in Ref. [26] for comparison. The circle and square symbols show the results obtained for $N_\tau = 16$ and 12, respectively, where N_τ is the number of lattice sites along the temporal direction which is related to the lattice spacing a as $N_\tau = (aT)^{-1}$.

From Fig. 9, one sees that our model results do not show good agreement with the lattice ones even qualitatively. In particular, while the lattice data show that the values of p_x and p_z hardly change from the one in the $L_x \rightarrow \infty$ limit for $L_x T \gtrsim 1.5$, this behavior is not reproduced in the model calculation. Similar results are obtained for other values of T/T_c investigated in Ref. [26]. Figure 10 compares these results in term of the pressure ratio p_x/p_z . From the figure one sees that the ratio obtained in our model is closer to unity than the massless-free result for $L_x T \gtrsim 2.0$, but the modification is not enough to reproduce the lattice results.

These results, however, show that the non-trivial expectation values of P_τ and P_x give non-negligible contribution to the behavior of thermodynamics on $\mathbb{T}^2 \times \mathbb{R}^2$. In

order to gain insights into their effects, we perform an additional analysis, where the values of P_x and P_τ are fixed by hand to those at $L_x \rightarrow \infty$; $P_\tau \approx 0.973$ and $P_x = 0$. The obtained results for ϵ , p_x and p_z are shown in Figs. 9 and 10 by the dashed lines. As can be seen, these results are insensitive to $L_x T$ and give consistent behavior with the lattice data for $L_x T \gtrsim 1.5$. These results show that P_x and P_τ affect thermodynamic quantities on $\mathbb{T}^2 \times \mathbb{R}^2$ significantly. Therefore, although we have failed in reproducing the lattice data in the present study with a simple model, the modification of the model, especially the potential term, would give a consistent result with the lattice data. Such a description of the lattice results on $\mathbb{T}^2 \times \mathbb{R}^2$ will in turn give us deeper understanding on the non-perturbative aspects of YM theory near T_c^∞ not only on $\mathbb{T}^2 \times \mathbb{R}^2$ but also $\mathbb{S}^1 \times \mathbb{R}^3$.

V. CONCLUSION AND OUTLOOK

In this paper, we have investigated the phase structure and thermodynamics of the pure Yang-Mills (YM) theory on $\mathbb{T}^2 \times \mathbb{R}^2$ with the PBC by means of an effective model. The model has two Polyakov loops along the compactified directions, P_τ and P_x , as the order parameters and thus is capable of describing the phase transitions associated with two Z_N symmetries. As a first investigation of such an effective model, we have employed a simple form for the potential term f_{pot} given by an extension of Ref. [34]. We have found that a rich phase structure on the L_τ - L_x plane can manifest itself due to two phase transitions, and the phase structure is qualitatively dependent on N .

The energy density and anisotropic pressure are also calculated in the model and are compared with the lattice results in Ref. [26]. Although we have found that our model fails in reproducing the lattice results, we have also found that thermodynamics on $\mathbb{T}^2 \times \mathbb{R}^2$ is sensitive to P_τ and P_x in the model. Therefore, while the present model with a simple ansatz is not satisfactory, the modification of the model would be able to reproduce the lattice results. The analysis in the previous section that fixes the values of P_τ and P_x by hand would be used for a guide for such a study. We also note that the model can be improved toward other directions, for example, introduction of the quasi-particle mass of the gauge field and other mean fields [40–48] especially mimicking the magnetic condensates in the deconfined phase [49]. Comparison with the stress tensor obtained in the AdS/CFT correspondence [50, 51] is also interesting to investigate the role of the strong-coupling nature.

The investigation of the field theory with the BC can also be extended to various directions. An example is the use of other BCs such as the anti-periodic BC in place of the PBC. Although we have limited our attention only to $N = 2, 3$, the study of N dependence for $N \geq 4$ is a straightforward extension of the present study. Similar analysis in QCD with dynamical fermions is another important subject. Since the measurement of thermody-

namics in QCD on $\mathbb{T}^2 \times \mathbb{R}^2$ is possible using the technique developed in Refs. [52–54], the comparison with the lattice data is possible.

ACKNOWLEDGEMENT

The authors thank Kouji Kashiwa, Makoto Natsuume and Yuya Tanizaki for giving us useful comments. This work is supported by the RIKEN special postdoctoral researcher program (D. S.), and JSPS KAKENHI Grant Numbers JP19H05598, JP20H01903, JP22K03619 (M. K.).

Appendix A: DERIVATION OF EQS. (15) and (16)

In this appendix we show derivation of Eqs. (15) and (16).

For $N = 2$, choosing the phase variables as Eq. (9), the non vanishing $(\Delta\theta_c)_{jk}$ reads

$$(\Delta\theta_c)_{12} = -(\Delta\theta_c)_{21} = 2\phi_c. \quad (\text{A1})$$

Hence, the one-loop free energy (13) is of the form

$$\begin{aligned} f_{\text{pert}} &= \frac{1}{L_\tau L_x} \sum_{l_\tau, l_x} \int \frac{d^2 p_L}{(2\pi)^2} \ln(\omega_\tau^2 + \omega_x^2 + \mathbf{p}_L^2) \\ &+ \frac{2}{L_\tau L_x} \sum_{l_\tau, l_x} \int \frac{d^2 p_L}{(2\pi)^2} \\ &\times \ln \left[\left(\omega_\tau - \frac{2\phi_\tau}{L_\tau} \right)^2 + \left(\omega_x - \frac{2\phi_x}{L_x} \right)^2 + \mathbf{p}_L^2 \right], \end{aligned} \quad (\text{A2})$$

with $\mathbf{p}_L = (p_y, p_z)$, $\omega_\tau = 2\pi l_\tau$ and $\omega_x = 2\pi l_x$ (l_τ and l_x are integers). Here, with the help of regularization procedures provided in detail in Appendix B, the one-loop free energy f_{pert} is appropriately regularized to be

$$\begin{aligned} f_{\text{pert}} &= -\frac{1}{2\pi^2} \overline{\sum}_{l_\tau, l_x} \frac{m^2}{X_{l_\tau, l_x}^2} K_2(mX_{l_\tau, l_x}) \\ &\times (1 + 2e^{2i\phi_\tau l_\tau} e^{2i\phi_x l_x}) \Big|_{m \rightarrow 0}. \end{aligned} \quad (\text{A3})$$

The symbol $\overline{\sum}_{l_\tau, l_x}$ in Eq. (A3) is defined such that the summation does not include contributions from $(l_\tau, l_x) = (0, 0)$. $K_y(x)$ in Eq. (A3) is the modified Bessel function of the second kind, and we have defined

$$X_{l_\tau, l_x} \equiv \sqrt{(l_\tau L_\tau)^2 + (l_x L_x)^2}. \quad (\text{A4})$$

It should be noted that we have included the mass of the gauge field m for convenience, but soon we take $m \rightarrow 0$. That is, using $K_2(x) \approx 2/x^2$ for $x \approx 0$, the free

energy (A3) is reduced to

$$\begin{aligned}
f_{\text{pert}} &= -\frac{1}{\pi^2} \sum_{l_\tau, l_x} \frac{1 + 2e^{2i\phi_\tau l_\tau} e^{2i\phi_x l_x}}{X_{l_\tau, l_x}^4} \\
&= -\frac{2}{\pi^2} \left[\sum_{l_\tau=1}^{\infty} \frac{1 + 2\cos(2\phi_\tau l_\tau)}{X_{l_\tau, 0}^4} \right. \\
&\quad + \sum_{l_x=1}^{\infty} \frac{1 + 2\cos(2\phi_x l_x)}{X_{0, l_x}^4} \\
&\quad \left. + 2 \sum_{l_\tau, l_x=1}^{\infty} \frac{1 + 2\cos(2\phi_\tau l_\tau) \cos(2\phi_x l_x)}{X_{l_\tau, l_x}^4} \right]. \quad (\text{A5})
\end{aligned}$$

The first and second lines in the second equality in Eq. (A5) are separate contributions from the compactified τ and x directions, respectively, while the third one contains interplays between them leading to a rich phase structure of the $Z_2^{(\tau)} \times Z_2^{(x)}$ on $\mathbb{T}^2 \times \mathbb{R}^2$. The separate contributions are reduced to rather familiar forms. In fact, the summations are rewritten by the Bernoulli polynomial by the following infinite series:

$$B_{2n}(x) = (-1)^{n+1} \frac{2(2n)!}{(2\pi)^{2n}} \sum_{k=1}^{\infty} \frac{\cos(2\pi kx)}{k^{2n}}, \quad (\text{A6})$$

with $0 \leq x \leq 1$, leading to

$$\begin{aligned}
f_{\text{pert}} &= \frac{2\pi^2}{3L_\tau^4} \left[B_4(0) + 2B_4(\phi_\tau/\pi) \right] \\
&\quad + \frac{2\pi^2}{3L_x^4} \left[B_4(0) + 2B_4(\phi_x/\pi) \right] \\
&\quad - \frac{4}{\pi^2} \sum_{l_\tau, l_x=1}^{\infty} \frac{1 + 2\cos(2\phi_\tau l_\tau) \cos(2\phi_x l_x)}{X_{l_\tau, l_x}^4}. \quad (\text{A7})
\end{aligned}$$

Therefore, remembering the elementary expression of the Bernoulli polynomial

$$B_4(x) = x^2(x-1)^2 - \frac{1}{30}, \quad (\text{A8})$$

we finally arrive at Eq. (15).

For $N = 3$, the parametrization in Eq. (11) enables us to rewrite the one-loop free energy (13) into

$$\begin{aligned}
f_{\text{pert}} &= \frac{2}{L_\tau L_x} \sum_{l_\tau, l_x} \int \frac{d^2 p_L}{(2\pi)^2} \ln(\omega_\tau^2 + \omega_x^2 + \mathbf{p}_L^2) \\
&\quad + \frac{4}{L_\tau L_x} \sum_{l_\tau, l_x} \int \frac{d^2 p_L}{(2\pi)^2} \\
&\quad \times \ln \left[\left(\omega_\tau - \frac{\phi_\tau}{L_\tau} \right)^2 + \left(\omega_x - \frac{\phi_x}{L_x} \right)^2 + \mathbf{p}_L^2 \right] \\
&\quad + \frac{2}{L_\tau L_x} \sum_{l_\tau, l_x} \int \frac{d^2 p_L}{(2\pi)^2} \\
&\quad \times \ln \left[\left(\omega_\tau - \frac{2\phi_\tau}{L_\tau} \right)^2 + \left(\omega_x - \frac{2\phi_x}{L_x} \right)^2 + \mathbf{p}_L^2 \right]. \quad (\text{A9})
\end{aligned}$$

Thus, tracing a similar evaluation from Eq. (A3) to Eq. (A7), one can straightforwardly obtain Eq. (16).

Next, we take a closer look at the $L_x/L_\tau \rightarrow \infty$ limit of f_{pert} focusing on the case $N = 2$; the generalization to arbitrary N is straightforward. As discussed in the text, the leading term in this limit is proportional to $1/L_\tau^4$ and it reproduces the result in Ref. [34]. The subleading term with respect to $r = L_\tau/L_x$ comes from the double-sum term in Eq. (15) or (A7). The expansion of this term with respect to r is cumbersome because a simple Taylor expansion of the denominator leads to divergent series. To suppress the divergence, one may first rewrite the double sum as

$$\begin{aligned}
&\sum_{l_\tau, l_x=1}^{\infty} \frac{1 + 2\cos(2\phi_\tau l_\tau) \cos(2\phi_x l_x)}{X_{l_\tau, l_x}^4} \\
&= \frac{1}{L_\tau^4} \sum_{l_\tau, l_x=1}^{\infty} \frac{1 + 2\cos(2\phi_\tau l_\tau) \cos(2\phi_x l_x)}{(l_\tau^2 + l_x^2/r^2)^2}. \quad (\text{A10})
\end{aligned}$$

Here, we show a useful identity

$$\begin{aligned}
&\sum_{l=1}^{\infty} \frac{\cos(2\phi l)}{(l^2 + C^2)^2} = \frac{1}{2} \sum_{l=-\infty}^{\infty} \frac{e^{2i\phi l}}{(l^2 + C^2)^2} - \frac{1}{2C^4} \\
&= \pi \sum_{m=-\infty}^{\infty} \frac{1 + 2C|\pi m + \phi|}{4C^3} e^{-2C|\pi m + \phi|} - \frac{1}{2C^4}, \quad (\text{A11})
\end{aligned}$$

which can be derived by the Poisson summation formula $\sum_{n=-\infty}^{\infty} F(n) = \sum_{m=-\infty}^{\infty} \tilde{F}(m)$ for $\tilde{F}(k) = \int_{-\infty}^{\infty} dx e^{i2\pi kx} F(x)$ with $F(x) = e^{2i\phi x} (x^2 + C^2)^{-2}$. For positive and sufficiently large C , the first term in Eq. (A11) is negligible due to the exponential term unless $\phi = 0$ so that the term is of the order C^{-4} for $\phi \neq 0$. Only when $\phi = 0$, non-vanishing contribution survives from $m = 0$ and Eq. (A11) becomes of order C^{-3} . Applying the identity (A11) to the summation with respect to l_τ in Eq. (A10) and focusing on a large value of $C = l_x/r$ together with the above order estimates, one can show that Eq. (A10) starts from $\mathcal{O}(r^3)$ where the remaining summation for l_x is converging. Therefore, the counting in Eq. (18) is derived.

Appendix B: REGULARIZATION BY THE EPSTEIN-HURWITZ ZETA FUNCTION

When evaluating the one-loop free energy, we encounter the following function:

$$\begin{aligned}
\mathcal{I} &\equiv \frac{1}{L_\tau L_x} \sum_{l_\tau, l_x} \int \frac{d^2 p_L}{(2\pi)^2} \\
&\quad \times \ln \left[(\omega_\tau - a_\tau)^2 + (\omega_x - a_x)^2 + \mathbf{p}_L^2 + m^2 \right]. \quad (\text{B1})
\end{aligned}$$

The function (B1) includes UV divergences. In this appendix, we show our method to regularize the divergences

by means of the inhomogeneous and generalized Epstein-Hurwitz zeta function together with the dimensional regularization [55].

To begin with, we perform the momentum integrals in Eq. (B1) as

$$\begin{aligned} \mathcal{I} &= -\frac{1}{L_\tau L_x} \sum_{l_\tau, l_x} \int \frac{d^d p_L}{(2\pi)^d} \\ &\times \frac{\partial}{\partial s} \left\{ \frac{1}{[(\omega_\tau - a_\tau)^2 + (\omega_x - a_x)^2 + \mathbf{p}_L^2 + m^2]^s} \right\} \Big|_{s \rightarrow 0} \\ &= -\frac{1}{L_\tau L_x} \frac{1}{(4\pi)^{d/2}} \frac{\partial}{\partial s} \left\{ \frac{\Gamma[s - \frac{d}{2}] E(s)}{\Gamma[s]} \right\} \Big|_{s \rightarrow 0}, \quad (\text{B2}) \end{aligned}$$

where $d = 2 - \epsilon$ and $E(s)$ is the inhomogeneous and generalized Epstein-Hurwitz zeta function of the form

$$E(s) = \sum_{l_\tau, l_x} \left[\frac{1}{(\omega_\tau - a_\tau)^2 + (\omega_x - a_x)^2 + m^2} \right]^{s - \frac{d}{2}}. \quad (\text{B3})$$

Although the summations in $E(s)$ are diverging when we take $s \rightarrow 0$, we utilize the following identity to rearrange the summations in terms of the modified Bessel function of the second kind:

$$\begin{aligned} &\sum_{n_1, \dots, n_N} \left[\frac{1}{w_1(n_1 - \alpha_1)^2 + \dots + w_N(n_N - \alpha_N)^2 + c^2} \right]^\nu \\ &= \frac{\pi^{N/2}}{\sqrt{w_1 \dots w_N}} \frac{\Gamma[\nu - \frac{N}{2}]}{\Gamma[\nu]} |c|^{N-2\nu} + \frac{\pi^\nu}{\sqrt{w_1 \dots w_N}} \frac{2}{\Gamma[\nu]} \\ &\times \sum_{n_1, \dots, n_N} \exp[2\pi i(n_1 \alpha_1 + \dots + n_N \alpha_N)] \\ &\times |c|^{\frac{N}{2} - \nu} \left[\frac{n_1^2}{w_1} + \dots + \frac{n_N^2}{w_N} \right]^{\frac{1}{2}(\nu - \frac{N}{2})} \\ &\times K_{\frac{N}{2} - \nu} \left(2\pi |c| \left[\frac{l_1^2}{w_1} + \dots + \frac{l_N^2}{w_N} \right]^{1/2} \right), \quad (\text{B4}) \end{aligned}$$

with n_1, \dots, n_N being integers. The symbol \sum_{n_1, \dots, n_N} in Eq. (B4) is defined such that the summation does not include contributions from $(n_1, \dots, n_N) = (0, \dots, 0)$. The rearrangement is useful to separate the diverging parts. Thanks to Eq. (B4), the $\Gamma[s - \frac{d}{2}]E(s)$ part in Eq. (B2) becomes finite as long as we keep ϵ finite even when $s \rightarrow 0$ is taken. Here, using $\Gamma[s] \approx 1/s - \gamma_E + \mathcal{O}(s)$ with the Euler's constant $\gamma_E = 0.577 \dots$, we can get

$$\begin{aligned} \frac{\partial}{\partial s} \left\{ \frac{\Gamma[s - \frac{d}{2}] E(s)}{\Gamma[s]} \right\} &= \frac{\partial}{\partial s} \left\{ s \Gamma \left[s - \frac{d}{2} \right] E(s) + \dots \right\} \\ &\stackrel{s \rightarrow 0}{\equiv} \Gamma \left[-\frac{d}{2} \right] E(0). \quad (\text{B5}) \end{aligned}$$

Therefore, from Eqs. (B4) and (B5), the function (B2) is

regularized and evaluated as

$$\begin{aligned} \mathcal{I} &= -\frac{1}{L_\tau L_x} \frac{1}{(4\pi)^{d/2}} \Gamma \left[-\frac{d}{2} \right] E(0) \\ &= \frac{1}{(4\pi)^{(d+2)/2}} \Gamma \left[-\frac{d+2}{2} \right] \left(\frac{1}{m^2} \right)^{-(d+2)/2} \\ &+ \frac{1}{2\pi^2} \sum_{l_\tau, l_x} \frac{m^2}{X_{l_\tau, l_x}^2} e^{i(l_\tau L_\tau a_\tau + l_x L_x a_x)} K_2(m X_{l_\tau, l_x}). \quad (\text{B6}) \end{aligned}$$

Remembering $d = 2 - \epsilon$, the first term in Eq. (B6) coincides with the result in vacuum within the ordinary dimensional regularization, implying that the UV divergences are appropriately regularized. Thus, the second term in Eq. (B6) is well-defined and must be understood as contributions from PBC. Obviously, such a clear separation is successfully done by use of the identity (B4).

Appendix C: GINZBURG-LANDAU ANALYSIS

Here, we make use of the Ginzburg-Landau theory to delineate the order of the phase transitions found in Sec. III.

First, we focus on the free energy for $N = 2$ where the free energy per unit volume is given by Eqs. (15) and (26). We change the phase variables ϕ_τ and ϕ_x to

$$\psi_\tau \equiv \frac{\pi}{2} - \phi_\tau, \quad \psi_x \equiv \frac{\pi}{2} - \phi_x, \quad (\text{C1})$$

such that $\psi_\tau = 0$ and $\psi_x = 0$ correspond to the $Z_2^{(\tau)}$ and $Z_2^{(x)}$ symmetric phases, respectively. Substituting Eq. (C1) to Eqs. (15) and (26), f is expressed in terms of ψ_τ and ψ_x as

$$\begin{aligned} f &= -\frac{\pi^2}{15L_\tau^4} + \frac{1}{12\pi^2 L_\tau^4} (\pi^2 - 4\psi_\tau^2)^2 \\ &- \frac{\pi^2}{15L_x^4} + \frac{1}{12\pi^2 L_x^4} (\pi^2 - 4\psi_x^2)^2 \\ &- \frac{4}{\pi^2} \sum_{l_\tau, l_x=1}^{\infty} \frac{1 + 2(-1)^{l_\tau + l_x} \cos(2\psi_\tau l_\tau) \cos(2\psi_x l_x)}{X_{l_\tau, l_x}^4} \\ &- \frac{1}{L_\tau R^3} \ln(\cos^2 \psi_\tau) - \frac{1}{L_x R^3} \ln(\cos^2 \psi_x). \quad (\text{C2}) \end{aligned}$$

By expanding the free energy (C2) around $\psi_c = 0$, one can investigate the critical behavior.

When taking $L_x \rightarrow \infty$, the second and third lines of Eq. (C2) are negligible. The free energy thus includes only ψ_τ and can be expanded as

$$\begin{aligned} f &= \frac{\pi^2}{60L_\tau^4} + \left(\frac{1}{L_\tau R^3} - \frac{2}{3L_\tau^4} \right) \psi_\tau^2 \\ &+ \left(\frac{4}{3\pi^2 L_\tau^4} + \frac{1}{6L_\tau R^3} \right) \psi_\tau^4 + \frac{2}{45L_\tau R^3} \psi_\tau^6 + \dots. \quad (\text{C3}) \end{aligned}$$

In this expansion, contributions of $\mathcal{O}(\psi_\tau^6)$ stems from the logarithms in the last line in Eq. (C2), and thanks to cosines there remain only terms having even powers of ψ_τ with positive coefficients. Hence, only the coefficient of ψ_τ^2 in Eq. (C3) can change its sign. For this reason we can conclude that the second-order phase transition takes place at

$$L_\tau = \left(\frac{2}{3}\right)^{1/3} R \approx 0.874R. \quad (\text{C4})$$

Next we consider the symmetric case $L \equiv L_\tau = L_x$. Assuming that $\psi \equiv \psi_\tau = \psi_x$, the free energy (C2) is expanded as

$$\begin{aligned} f &= \left(\frac{\pi^2}{30L^4} - \frac{4}{\pi^2 L^4} \sum_{l_\tau, l_x} \frac{1 + 2(-1)^{l_\tau + l_x}}{(l_\tau^2 + l_x^2)^2} \right) \\ &+ \left(\frac{2}{LR^3} - \frac{4}{3L^4} + \frac{16}{\pi^2 L^4} \sum_{l_\tau, l_x} \frac{(-1)^{l_\tau + l_x}}{l_\tau^2 + l_x^2} \right) \psi^2 \\ &+ \dots \end{aligned} \quad (\text{C5})$$

Using

$$\sum_{l_\tau, l_x} \frac{(-1)^{l_\tau + l_x}}{l_\tau^2 + l_x^2} = \frac{\pi^2 - 3\pi \ln 2}{12}, \quad (\text{C6})$$

the coefficient of ψ^2 in Eq. (C5) is calculated to be

$$\frac{2}{L^4} \left(-\frac{2}{\pi} \ln 2 + \frac{L^3}{R^3} \right). \quad (\text{C7})$$

Since the sign of Eq. (C7) changes at $L = (2 \ln 2 / \pi)^{1/3} R$, if the phase transition is of second order the critical value of L is given by this value. As in the text, this assumption is supported numerically.

Let us consider the fate of the second-order transition line that separates $\phi_x = 0$ and $\phi_x \neq 0$ (the red line in Fig. 4) in the limit $(L_\tau, L_x) \rightarrow (0, \infty)$. Assuming the second-order phase transition, this line is given by

$$\frac{\partial^2 f}{\partial \psi_x^2} \Big|_{\psi_x=0} = \frac{\partial^2 f_{\text{pert}}}{\partial \psi_x^2} \Big|_{\psi_x=0} + \frac{\partial^2 f_{\text{pot}}}{\partial \psi_x^2} \Big|_{\psi_x=0} = 0. \quad (\text{C8})$$

Since $P_\tau = 1$ and thus $\psi_\tau = \pi/2$ is satisfied in this limit, the asymptotic form of $\partial^2 f_{\text{pert}} / \partial \psi_x^2 |_{\psi_x=0}$ is calculated to be

$$\begin{aligned} \frac{\partial^2 f_{\text{pert}}}{\partial \psi_x^2} \Big|_{\psi_x=0} &= \frac{32}{\pi^2 L_\tau^4} \sum_{l_\tau, l_x=1}^{\infty} \frac{(-1)^{l_x} l_x^2}{(l_\tau^2 + l_x^2 / r^2)^2} \\ &= \frac{8}{L_\tau^4} \sum_{l_x=1}^{\infty} (-1)^{l_x} \left(r^2 \sinh^{-2} \frac{l_x \pi}{r} + \frac{r^3}{\pi l_x} \coth \frac{l_x \pi}{r} - \frac{2}{\pi^2} \frac{r^4}{l_x^2} \right) \\ &\xrightarrow{r \rightarrow 0} \frac{8}{\pi} \frac{1}{L_\tau L_x^3} \sum_{l_x=1}^{\infty} \frac{(-1)^{l_x}}{l_x} = -\frac{8}{\pi} \ln(2) \frac{1}{L_\tau L_x^3}, \end{aligned} \quad (\text{C9})$$

with $r = L_\tau / L_x$. Since $\partial^2 f_{\text{pot}} / \partial \psi_x^2 |_{\psi_x=0} = 2 / L_x R^3$, Eq. (C8) is satisfied at

$$L_\tau = \frac{4 \ln(2)}{\pi} \frac{R^3}{L_x^2} \simeq 0.8825 \frac{R^3}{L_x^2}. \quad (\text{C10})$$

Next, we focus on the free energy for $N = 3$ given by Eqs. (16) and (27). Changing the variables as

$$\psi_\tau \equiv \frac{2\pi}{3} - \phi_\tau, \quad \psi_x \equiv \frac{2\pi}{3} - \phi_x \quad (\text{C11})$$

such that $\psi_c = 0$ corresponds to $P_c = 0$, the free energy reads

$$\begin{aligned} f &= \frac{8\pi^2}{405L_\tau^4} - \frac{2}{3L_\tau^4} \psi_\tau^2 - \frac{2}{3\pi L_\tau^4} \psi_\tau^3 + \frac{3}{2\pi^2 L_\tau^4} \psi_\tau^4 \\ &+ \frac{8\pi^2}{405L_x^4} - \frac{2}{3L_x^4} \psi_x^2 - \frac{2}{3\pi L_x^4} \psi_x^3 + \frac{3}{2\pi^2 L_x^4} \psi_x^4 \\ &+ \dots \end{aligned} \quad (\text{C12})$$

That is, the free energy always includes cubic terms of ψ_τ and ψ_x with negative coefficients, generally resulting in a first-order phase transition. It is easily shown that the negative cubic terms also appear for $N \geq 3$. For this reason we infer that the first-order phase transitions and phase diagrams similar to Fig. 8 are universally obtained for $N \geq 3$.

-
- [1] H. B. G. Casimir, "On the Attraction Between Two Perfectly Conducting Plates," *Indag. Math.* **10**, 261–263 (1948).
- [2] S. K. Lamoreaux, "Demonstration of the Casimir force in the 0.6 to 6 micrometers range," *Phys. Rev. Lett.* **78**, 5–8 (1997), [Erratum: *Phys. Rev. Lett.* **81**, 5475–5476 (1998)].
- [3] U. Mohideen and Anushree Roy, "Precision measurement of the Casimir force from 0.1 to 0.9 micrometers," *Phys. Rev. Lett.* **81**, 4549–4552 (1998), [arXiv:physics/9805038](https://arxiv.org/abs/physics/9805038).
- [4] Benjamin Svetitsky and Laurence G. Yaffe, "Critical Behavior at Finite Temperature Confinement Transitions," *Nucl. Phys. B* **210**, 423–447 (1982).
- [5] Alexander M. Polyakov, "Thermal Properties of Gauge Fields and Quark Liberation," *Phys. Lett. B* **72**, 477–480 (1978).
- [6] Dusan Simic and Mithat Unsal, "Deconfinement in Yang-Mills theory through toroidal compactification with deformation," *Phys. Rev. D* **85**, 105027 (2012), [arXiv:1010.5515 \[hep-th\]](https://arxiv.org/abs/1010.5515).
- [7] B. C. Tiburzi, "Chiral Symmetry Restoration from a Boundary," *Phys. Rev. D* **88**, 034027 (2013), [arXiv:1302.6645 \[hep-lat\]](https://arxiv.org/abs/1302.6645).
- [8] Antonino Flachi, "Strongly Interacting Fermions and Phases of the Casimir Effect," *Phys. Rev. Lett.* **110**, 060401 (2013), [arXiv:1301.1193 \[hep-th\]](https://arxiv.org/abs/1301.1193).
- [9] Eduardo S. Fraga, Daniel Kroff, and Jorge Noronha,

- “Linde problem in Yang-Mills theory compactified on $\mathbb{R}^2 \times \mathbb{T}^2$,” *Phys. Rev. D* **95**, 034031 (2017), [arXiv:1610.01130 \[hep-th\]](#).
- [10] Dimitra Karabali and V. P. Nair, “Casimir effect in (2+1)-dimensional Yang-Mills theory as a probe of the magnetic mass,” *Phys. Rev. D* **98**, 105009 (2018), [arXiv:1808.07979 \[hep-th\]](#).
- [11] Sylvain Mogliacci, Isobel Kolbé, and W. A. Horowitz, “Geometrically confined thermal field theory: Finite size corrections and phase transitions,” *Phys. Rev. D* **102**, 116017 (2020), [arXiv:1807.07871 \[hep-th\]](#).
- [12] Tsutomu Ishikawa, Katsumasa Nakayama, and Kei Suzuki, “Casimir effect for nucleon parity doublets,” *Phys. Rev. D* **99**, 054010 (2019), [arXiv:1812.10964 \[hep-ph\]](#).
- [13] A. F. Santos and Faqir C. Khanna, “Casimir effect and Stefan-Boltzmann law in Yang-Mills theory at finite temperature,” *Int. J. Mod. Phys. A* **34**, 1950128 (2019), [arXiv:1907.12534 \[hep-th\]](#).
- [14] Tsutomu Ishikawa, Katsumasa Nakayama, Daiki Suenaga, and Kei Suzuki, “ D mesons as a probe of Casimir effect for chiral symmetry breaking,” *Phys. Rev. D* **100**, 034016 (2019), [arXiv:1905.11164 \[hep-ph\]](#).
- [15] Tsutomu Ishikawa, Katsumasa Nakayama, and Kei Suzuki, “Casimir effect for lattice fermions,” *Phys. Lett. B* **809**, 135713 (2020), [arXiv:2005.10758 \[hep-lat\]](#).
- [16] Tsutomu Ishikawa, Katsumasa Nakayama, and Kei Suzuki, “Lattice-fermionic Casimir effect and topological insulators,” *Phys. Rev. Res.* **3**, 023201 (2021), [arXiv:2012.11398 \[hep-lat\]](#).
- [17] David Dudal, Pablo Pais, and Luigi Rosa, “Casimir energy in terms of boundary quantum field theory: The QED case,” *Phys. Rev. D* **102**, 016026 (2020), [arXiv:2005.12693 \[hep-th\]](#).
- [18] Tomohiro Inagaki, Yamato Matsuo, and Hiromu Shimoji, “Precise phase structure in a four-fermion interaction model on a torus,” *PTEP* **2022**, 013B09 (2022), [arXiv:2108.03583 \[hep-ph\]](#).
- [19] Xingyu Guo, Jiaying Zhao, and Pengfei Zhuang, “Casimir effect in kinetic theory,” (2022), [arXiv:2202.13537 \[quant-ph\]](#).
- [20] M. N. Chernodub, “Rotating Casimir systems: magnetic-field-enhanced perpetual motion, possible realization in doped nanotubes, and laws of thermodynamics,” *Phys. Rev. D* **87**, 025021 (2013), [arXiv:1207.3052 \[quant-ph\]](#).
- [21] M. N. Chernodub, V. A. Goy, and A. V. Molochkov, “Casimir effect on the lattice: $U(1)$ gauge theory in two spatial dimensions,” *Phys. Rev. D* **94**, 094504 (2016), [arXiv:1609.02323 \[hep-lat\]](#).
- [22] M. N. Chernodub, V. A. Goy, and A. V. Molochkov, “Nonperturbative Casimir effect and monopoles: compact Abelian gauge theory in two spatial dimensions,” *Phys. Rev. D* **95**, 074511 (2017), [arXiv:1703.03439 \[hep-lat\]](#).
- [23] M. N. Chernodub, V. A. Goy, and A. V. Molochkov, “Casimir effect and deconfinement phase transition,” *Phys. Rev. D* **96**, 094507 (2017), [arXiv:1709.02262 \[hep-lat\]](#).
- [24] M. N. Chernodub, V. A. Goy, A. V. Molochkov, and Ha Huu Nguyen, “Casimir Effect in Yang-Mills Theory in $D=2+1$,” *Phys. Rev. Lett.* **121**, 191601 (2018), [arXiv:1805.11887 \[hep-lat\]](#).
- [25] M. N. Chernodub, V. A. Goy, and A. V. Molochkov, “Phase structure of lattice Yang-Mills theory on $\mathbb{T}^2 \times \mathbb{R}^2$,” *Phys. Rev. D* **99**, 074021 (2019), [arXiv:1811.01550 \[hep-lat\]](#).
- [26] Masakiyo Kitazawa, Sylvain Mogliacci, Isobel Kolbé, and W. A. Horowitz, “Anisotropic pressure induced by finite-size effects in $SU(3)$ Yang-Mills theory,” *Phys. Rev. D* **99**, 094507 (2019), [arXiv:1904.00241 \[hep-lat\]](#).
- [27] M. N. Chernodub, Harold Erbin, I. V. Grishmanovskii, V. A. Goy, and A. V. Molochkov, “Casimir effect with machine learning,” *Phys. Rev. Res.* **2**, 033375 (2020), [arXiv:1911.07571 \[hep-lat\]](#).
- [28] M. N. Chernodub, V. A. Goy, A. V. Molochkov, and A. S. Tanashkin, “Casimir boundaries, monopoles, and deconfinement transition in 3+1 dimensional compact electrodynamics,” (2022), [arXiv:2203.14922 \[hep-lat\]](#).
- [29] Hiroshi Suzuki, “Energy-momentum tensor from the Yang-Mills gradient flow,” *PTEP* **2013**, 083B03 (2013), [Erratum: *PTEP*2015, 079201 (2015)], [arXiv:1304.0533 \[hep-lat\]](#).
- [30] Masayuki Asakawa, Tetsuo Hatsuda, Etsuko Itou, Masakiyo Kitazawa, and Hiroshi Suzuki (FlowQCD), “Thermodynamics of $SU(3)$ gauge theory from gradient flow on the lattice,” *Phys. Rev. D* **90**, 011501 (2014), [Erratum: *Phys. Rev. D*92, no. 5, 059902 (2015)], [arXiv:1312.7492 \[hep-lat\]](#).
- [31] Masakiyo Kitazawa, Takumi Iritani, Masayuki Asakawa, Tetsuo Hatsuda, and Hiroshi Suzuki, “Equation of State for $SU(3)$ Gauge Theory via the Energy-Momentum Tensor under Gradient Flow,” *Phys. Rev. D* **94**, 114512 (2016), [arXiv:1610.07810 \[hep-lat\]](#).
- [32] Takumi Iritani, Masakiyo Kitazawa, Hiroshi Suzuki, and Hiromasa Takaura, “Thermodynamics in quenched QCD: energy-momentum tensor with two-loop order coefficients in the gradient flow formalism,” *PTEP* **2019**, 023B02 (2019), [arXiv:1812.06444 \[hep-lat\]](#).
- [33] Lowell S. Brown and G. Jordan Maclay, “Vacuum stress between conducting plates: An Image solution,” *Phys. Rev.* **184**, 1272–1279 (1969).
- [34] Peter N. Meisinger, Travis R. Miller, and Michael C. Ogilvie, “Phenomenological equations of state for the quark gluon plasma,” *Phys. Rev. D* **65**, 034009 (2002), [arXiv:hep-ph/0108009](#).
- [35] Robert D. Pisarski, “Quark gluon plasma as a condensate of $SU(3)$ Wilson lines,” *Phys. Rev. D* **62**, 111501 (2000), [arXiv:hep-ph/0006205](#).
- [36] Kenji Fukushima and Vladimir Skokov, “Polyakov loop modeling for hot QCD,” *Prog. Part. Nucl. Phys.* **96**, 154–199 (2017), [arXiv:1705.00718 \[hep-ph\]](#).
- [37] Heinz J. Rothe, *Lattice Gauge Theories : An Introduction (Fourth Edition)*, Vol. 43 (World Scientific Publishing Company, 2012).
- [38] L. G. Yaffe and B. Svetitsky, “First Order Phase Transition in the $SU(3)$ Gauge Theory at Finite Temperature,” *Phys. Rev. D* **26**, 963 (1982).
- [39] Benjamin Svetitsky, “Symmetry Aspects of Finite Temperature Confinement Transitions,” *Phys. Rept.* **132**, 1–53 (1986).
- [40] Francesco Sannino, “Polyakov loops versus hadronic states,” *Phys. Rev. D* **66**, 034013 (2002), [arXiv:hep-ph/0204174](#).
- [41] M. Ruggieri, P. Alba, P. Castorina, S. Plumari, C. Ratti, and V. Greco, “Polyakov Loop and Gluon Quasiparticles in Yang-Mills Thermodynamics,” *Phys. Rev. D* **86**, 054007 (2012), [arXiv:1204.5995 \[hep-ph\]](#).
- [42] Chihiro Sasaki and Krzysztof Redlich, “An Effective

- gluon potential and hybrid approach to Yang-Mills thermodynamics,” *Phys. Rev. D* **86**, 014007 (2012), [arXiv:1204.4330 \[hep-ph\]](#).
- [43] Chihiro Sasaki, Igor Mishustin, and Krzysztof Redlich, “Implementation of chromomagnetic gluons in Yang-Mills thermodynamics,” *Phys. Rev. D* **89**, 014031 (2014), [arXiv:1308.3635 \[hep-ph\]](#).
- [44] Mark I. Gorenstein and Shin-Nan Yang, “Gluon plasma with a medium dependent dispersion relation,” *Phys. Rev. D* **52**, 5206–5212 (1995).
- [45] A. Peshier, Burkhard Kampfer, O. P. Pavlenko, and G. Soff, “A Massive quasiparticle model of the SU(3) gluon plasma,” *Phys. Rev. D* **54**, 2399–2402 (1996).
- [46] G. W. Carter, O. Scavenius, I. N. Mishustin, and P. J. Ellis, “An Effective model for hot gluodynamics,” *Phys. Rev. C* **61**, 045206 (2000), [arXiv:nucl-th/9812014](#).
- [47] Fabian Brau and Fabien Buisseret, “Glueballs and statistical mechanics of the gluon plasma,” *Phys. Rev. D* **79**, 114007 (2009), [arXiv:0902.4836 \[hep-ph\]](#).
- [48] V. V. Begun, M. I. Gorenstein, and O. A. Mogilevsky, “Modified Bag Models for the Quark Gluon Plasma Equation of State,” *Int. J. Mod. Phys. E* **20**, 1805–1815 (2011), [arXiv:1004.0953 \[hep-ph\]](#).
- [49] Nikita O. Agasian, “Thermal gluomagnetic vacuum of SU(N) gauge theory,” *Phys. Lett. B* **562**, 257–264 (2003), [arXiv:hep-ph/0303127](#).
- [50] Vijay Balasubramanian and Per Kraus, “A Stress tensor for Anti-de Sitter gravity,” *Commun. Math. Phys.* **208**, 413–428 (1999), [arXiv:hep-th/9902121](#).
- [51] Robert C. Myers, “Stress tensors and Casimir energies in the AdS / CFT correspondence,” *Phys. Rev. D* **60**, 046002 (1999), [arXiv:hep-th/9903203](#).
- [52] Hiroki Makino and Hiroshi Suzuki, “Lattice energy–momentum tensor from the Yang–Mills gradient flow—inclusion of fermion fields,” *PTEP* **2014**, 063B02 (2014), [Erratum: PTEP 2015, 079202 (2015)], [arXiv:1403.4772 \[hep-lat\]](#).
- [53] Yusuke Taniguchi, Shinji Ejiri, Ryo Iwami, Kazuyuki Kanaya, Masakiyo Kitazawa, Hiroshi Suzuki, Takashi Umeda, and Naoki Wakabayashi, “Exploring $N_f = 2+1$ QCD thermodynamics from the gradient flow,” *Phys. Rev. D* **96**, 014509 (2017), [Erratum: Phys.Rev.D 99, 059904 (2019)], [arXiv:1609.01417 \[hep-lat\]](#).
- [54] Yusuke Taniguchi, Shinji Ejiri, Kazuyuki Kanaya, Masakiyo Kitazawa, Hiroshi Suzuki, and Takashi Umeda (WHOT-QCD), “ $N_f = 2+1$ QCD thermodynamics with gradient flow using two-loop matching coefficients,” *Phys. Rev. D* **102**, 014510 (2020), [Erratum: Phys.Rev.D 102, 059903 (2020)], [arXiv:2005.00251 \[hep-lat\]](#).
- [55] E. Elizalde, *Ten physical applications of spectral zeta functions*, Vol. 35 (1995).